

# Experimental Modeling, Repeatability Investigation and Optimization of Microwave Bond Wire Interconnects

Albert Sutono, *Member, IEEE*, N. Gio Cafaro, *Member, IEEE*, Joy Laskar, *Member, IEEE*, and Manos M. Tentzeris

**Abstract**—We present the first comprehensive experimental characterization of bond wire interconnects at microwave frequencies which includes a repeatability study, modeling and optimization. Wire bond interconnects with two different bond types (ball-crescent and wedge), two different loop types (tight and loose) and two different lengths (15 and 25 mils), were fabricated and experimentally investigated. We report the performance and repeatability comparison of these configurations and develop an electromagnetic as well as a simple wide band lumped-element equivalent circuit model to 40 GHz. A novel ribbon bond interconnect topology has also been proposed and experimentally tested demonstrating 65% less reflection compared to the conventional bond wire or ribbon configuration.

**Index Terms**—Bond wires, electrical modeling, microwave, microwave packaging.

## I. INTRODUCTION

**D**ESPITE the emergence of new packaging and interconnect technologies, wire-bonding remains the dominant conventional low cost, high reliability and high manufacturability chip connection technology [1]. When used in packaged microwave integrated circuits, wire bonds exhibit parasitic effects that impact the module performance. Bonding wire on air used as interconnect in a microwave module exhibits a high characteristic impedance [2] due to large inductance [3] caused by a typically thin wire diameter and small capacitance due to small air dielectric constant between the wire and the ground plane. In addition, radiation loss due to discontinuity [4] caused by wire bends on both ends of the wire, becomes significant, particularly in the millimeter wave frequency range [3]. Therefore, accurate high frequency characterization is critical to prevent considerable performance degradation.

Experimental [5], [6] and numerical [3], [7], [8] characterization typically neglect the variation in wire bond parameters such as the loop height or assume a particular configuration. In this paper, a comprehensive characterization of wire bond interconnects on air connecting two microstrip lines as a function of lengths, loop heights (tight and loose loops) and bond types (ball-crescent and wedge) is presented. Wide-band electrical

and electromagnetic models were developed for each configuration. A sensitivity analysis is also experimentally performed to study the effects of fabrication tolerances which include wire lengths and loop heights to the interconnect performance. A study based on the sensitivity analysis results is then performed to determine which configurations show more repeatable and better performance and its effect on the variation in the model parameter. Finally, a novel ribbon bond interconnect architecture is proposed to reduce the reflection caused by the high characteristic impedance typically encountered in the conventional ribbon and bond-wire configuration. Measurement results of this new topology show more than 65% less reflection and comparable insertion loss when compared to the conventional multiple wires and single ribbon configurations.

## II. DESIGN OF EXPERIMENTS

Microstrip bond wire test structures with a single one-mil diameter gold wire were manually fabricated using thermosonic ball and wedge bonders [1] on 10 mils thick Probe Point™ microstrip to coplanar waveguide on alumina substrates [11]. Such a configuration is desirable to enable on-wafer measurement using air coplanar probes. The wire-bond performance was investigated as a function of lengths, bond shapes (wedge and ball crescent) and loop heights (tight and loose). Several ball-crescent and wedge-wedge test structures fabricated with tight and loose wire loops and different lengths (15 and 25 mils) were placed on a gold plated brass used as a ground plane. For both bond styles, the tight loop configuration is approximately 20 mils high above the ground plane, while the maximum height of the loose loop wire is approximately 40 mils above the ground plane. The wire length mentioned here is approximately equal to the distance between the two adapters where the wire is bonded assuming the wire is tightly bonded. In the tight loop configuration, the wire was made as straight as possible. For loose loop configuration, the wire height is higher than that of the tight loop configuration and therefore, the wire length is longer. For both cases, the wires were bonded as close to the microstrip edge as possible such that the wire lengths are approximately the distance between the two adapters.

The adapters were attached on a gold-plated brass used as a ground plane using a conductive epoxy after which the microstrip ends of the adapters are wirebonded. TRL calibration [9], [10], [12] was performed from 1.5 GHz to 40 GHz to de-embed the adapters and establish the reference plane at the microstrip ends of the adapter so that the measured result contains only the wire bond under test.

Manuscript received September 10, 2000; revised November 1, 2001. This work was supported by NSF Career Award PRC ECS-9 623 964 and the NSF Packaging Research Center.

A. Sutono is with RF Solutions, Inc., Atlanta, GA 30332 USA.

N. G. Cafaro is with the Florida Communications Research Laboratory, Motorola Labs, Plantation, FL 33322 USA.

J. Laskar and M. M. Tentzeris are with the Packaging Research Center, School of Electrical and Computer Engineering, Georgia Institute of Technology, Atlanta, GA 30332-0250 USA (e-mail: gt8147a@prism.gatech.edu).

Publisher Item Identifier S 1521-3323(01)11182-2.

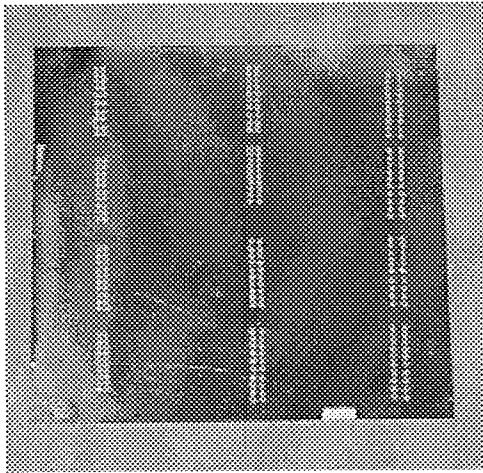


Fig. 1. Test board containing bond wire test structures.

Manufacturing tools used to fabricate microelectronic packaging interconnects have certain precision that affects the quality of the interconnects. Therefore, there are inherent nonidealities, tolerances and variations on the fabricated interconnects whose effects need to be carefully investigated. Given the fabrication tolerance, an investigation must be conducted to examine the effects on the interconnect performance especially at high frequencies. There is also a need to characterize quantitatively and predict the changes in performance given the upper and lower bound of tolerance specified by the manufacturer. The wire bonders have an inherent tolerance on the length of wire they can bond onto the substrate, the location of the bonds, as well as the loop height of the wire bond. The effects of the variations of these parameters on the performance of the interconnects are studied in detail.

To investigate the effect of fabrication tolerance to the wire bond performance, several identical structures for each configuration were fabricated. There are a total of eight groups with different configuration as functions of lengths (15 and 25 mils), loop heights (tight and loose) and bond types (ball-crescent and wedge). For each configuration, ten identical samples were fabricated to determine the variation in performance as well as the best and worst case performance. All the test samples were fabricated using microstrip to coplanar waveguide adapters on the same gold plated brass used as a ground plane and therefore, there are a total of 80 wire bond test samples to be characterized. Fig. 1 shows the photograph of the metalized board on which the test samples were attached. To ensure that the limitation set by the measurement test set does not affect the measured data significantly, multiple measurements have been conducted to verify the repeatability of the measurement data and the integrity of the measuring equipment.

### III. EXPERIMENTAL RESULTS

#### A. Ball-Crescent Wire Bonds

Figs. 2 and 3 show the measured magnitude of  $S_{11}$  and  $S_{21}$  of the 15 and 25 mil ball-crescent test structures with tight and loose loop configurations, respectively. As expected, the loose loop wires, in addition to exhibiting more loss, is also less repeatable by looking at the maximum variation of  $S_{11}$  and  $S_{21}$

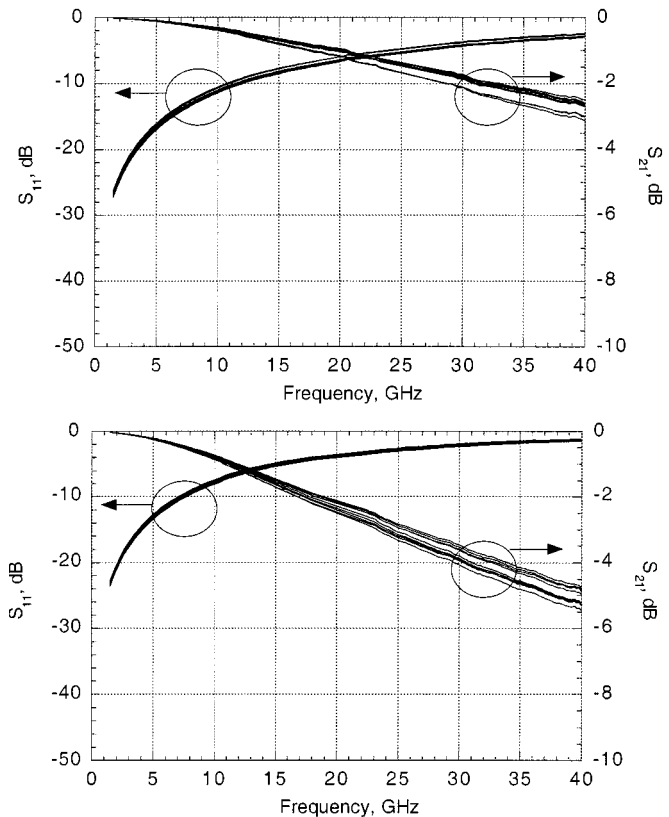


Fig. 2. Magnitude of  $S_{11}$  and  $S_{21}$  of ten 15 mil (top) and 25 mil (bottom) tight loop ball-crescent wire bonds.

in Figs. 2 and 3. The maximum variation of  $S_{11}$ ,  $\Delta S_{11}$  for the 15 and 25 mil tight ball crescent wires is 0.8 dB and 0.6 dB, respectively, while that of the loose loop is 1 dB and 0.9 dB for the 15 and 25 mil wires, respectively. The fact that the loose ball crescent is less repeatable can be observed more clearly by noting the maximum variation of the insertion loss  $\Delta S_{21}$ . The tight loop exhibits 0.6 dB  $\Delta S_{21}$  for both wire lengths while the loose loop shows 0.9 dB and 1 dB  $\Delta S_{21}$  for the 15 and 25 mil wire lengths, respectively, at 40 GHz. Therefore, the loose loop ball-crescent exhibits an average of 0.25 dB more  $\Delta S_{11}$  and 0.35 dB more  $\Delta S_{21}$  compared to the tight loop counterpart.

#### B. Wedge Wire Bonds

The performance variation of the wedge wire bonds is shown in Figs. 4 and 5. The loose loop configuration is also slightly less repeatable than the tight loop, in addition to showing larger insertion loss. As indicated in Fig. 4, the tight loop demonstrated 2.5 dB and 0.8 dB of  $\Delta S_{11}$ , 1.5 dB and 0.6 dB of  $\Delta S_{21}$  for the 15 and 25 mil wires, respectively. The loose loop shows 2 dB and 0.8 dB of  $\Delta S_{11}$ , 1.6 dB and 0.8 dB of  $\Delta S_{21}$  for the 15 and 25 mil wedge wires, respectively as shown in Fig. 5. While the  $\Delta S_{11}$  performance between the tight and loose loop is comparable, the loose loop wedge wires exhibit an average of 0.15 dB more  $\Delta S_{21}$  than the tight loop.

#### C. Comparison of Ball-Crescent and Wedge Wire Bonds

From the information of  $\Delta S_{11}$  and  $\Delta S_{21}$  derived from Fig. 2–5, it can be concluded that the wedge bond wire, despite its suitability for fine-pitch bonding, is less repeatable for short

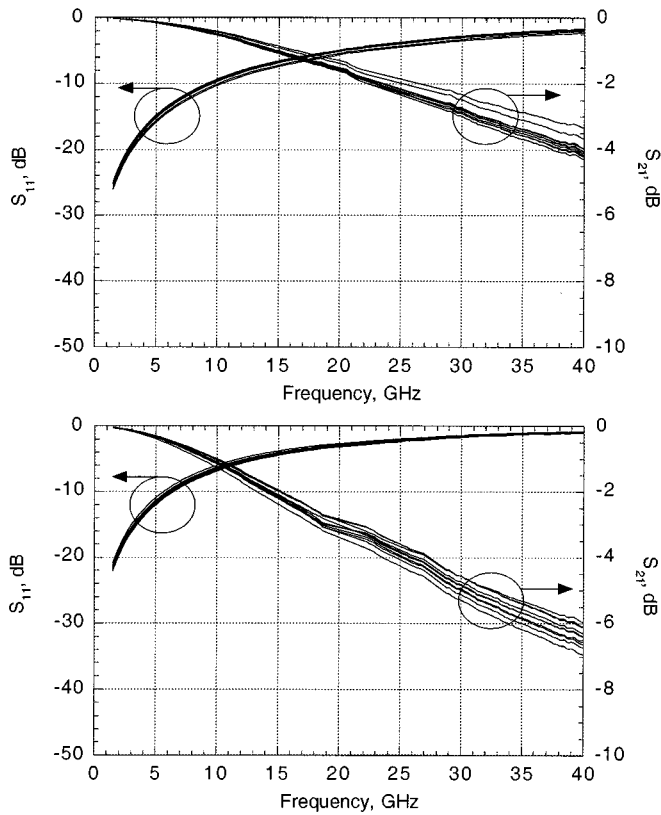


Fig. 3. Magnitude of  $S_{11}$  and  $S_{21}$  of ten 15 mil (top) and 25 mil (bottom) loose loop ball-crescent wire bonds.

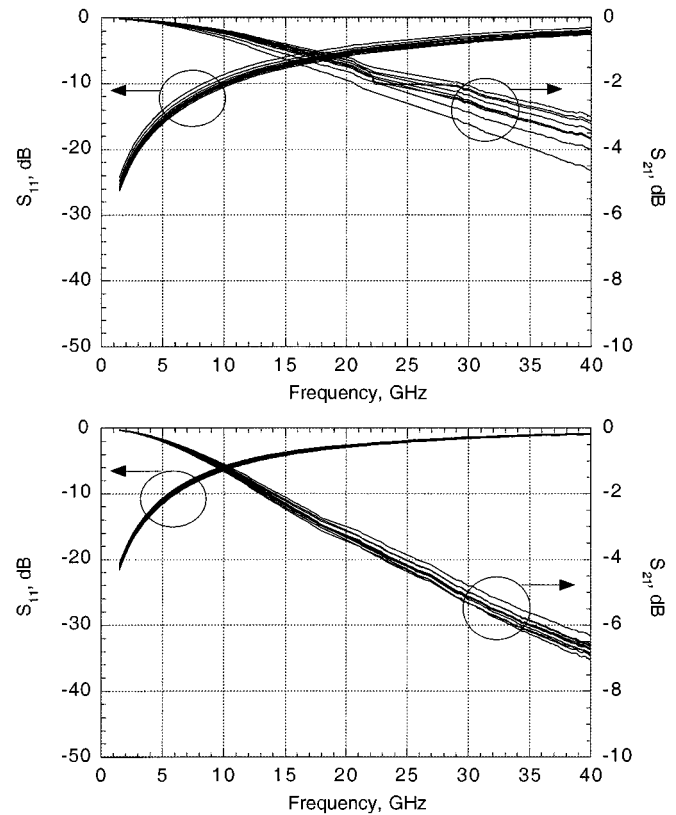


Fig. 5. Magnitude of  $S_{11}$  and  $S_{21}$  of ten 15 mil (top) and 25 mil (bottom) loose loop wedge wire bonds.

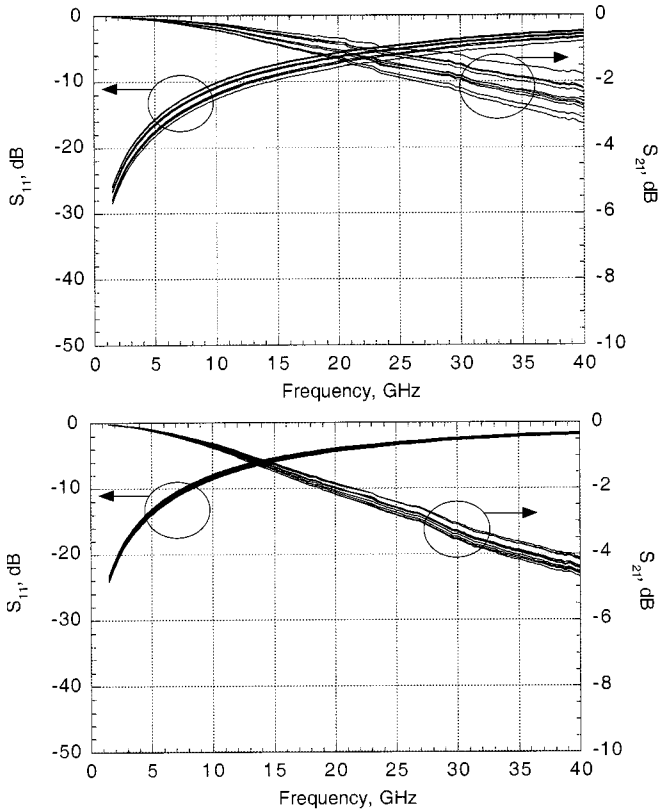


Fig. 4. Magnitude of  $S_{11}$  and  $S_{21}$  of ten 15 mil (top) and 25 mil (bottom) tight loop wedge wire bonds.

wires, which is true for both tight and loose loop configurations. For the 15 mil wires, the ball-crescent shows 0.6 dB and 0.9 dB

$\Delta S_{21}$  for tight and loose loop configurations, respectively. On the other hand, the wedge wires show 1.5 dB and 1.6 dB  $\Delta S_{21}$  for the tight and loose loop configurations, respectively. For the 25 mil wires, the ball-crescent shows 0.6 dB and 1 dB  $\Delta S_{21}$  for the tight and loose loops respectively, while the wedge demonstrates 0.6 dB and 0.8 dB  $\Delta S_{21}$  for tight and loose loop configurations, respectively. Therefore, for longer wires, which in this case is demonstrated by 25 mil wires, the repeatability of wedge wire bonds is comparable to that of ball crescent. Detailed summary of the performance variation of the eight groups of test structures is provided in Table I.

The ball bonder has the advantage to establish tight loop and short wire bond connection easier since the capillary does not have to be lifted up further once the ball bond has been generated and thus, allowing immediate stretching of the wire to be bonded at the other end. The wedge bonder, however, requires certain height before the wire can be stretched to the other end. The variation of height prior to stretching is a major source of wider range of performance variation exhibited by the wedge as compared to ball-crescent wire bonds.

#### IV. ELECTROMAGNETIC AND LUMPED ELEMENT ELECTRICAL MODEL

A number of electromagnetic (EM) models for wire bonds have been developed and custom numerical techniques have been implemented for analysis and characterization. EM simulations using custom finite difference in time domain [7], enhanced method of moments [3] and method of line [8] algorithms have been performed. We have developed a new EM

TABLE I  
PERFORMANCE VARIATION SUMMARY OF VARIOUS BOND-WIRE  
INTERCONNECT TEST STRUCTURES

Bond shape	Length (mils)	Loop Height	$\Delta S_{11,max}$ (dB)	$\Delta S_{21,max}$ (dB)	$\Delta S_{11,max}$ (degrees)	$\Delta S_{21,max}$ (degrees)
Ball-crescent	15	Tight	0.8	0.6	11	7
Ball-crescent	25	Tight	0.6	0.6	4	6
Ball-crescent	15	Loose	1	0.9	6	5
Ball-crescent	25	Loose	0.9	1	8	6
Wedge	15	Tight	2.5	1.5	12	14
Wedge	25	Tight	0.8	0.6	11	6
Wedge	15	Loose	2	1.6	14	14
Wedge	25	Loose	0.8	0.8	3.5	6

model for wire bond and simulated using a commercially available full-wave EM simulator by method of moment (MoM) [13], [14]. This model is implemented for two different wire bond lengths; 15 and 25 mils. The approximated geometry of a tight-loop wire bond is illustrated in Fig. 6(a).

In this figure,  $h_S$  and  $h_L$  indicate the thickness of the microstrip substrate onto which the wire is bonded and the wire height above the ground plane, respectively. Fig. 6(b) shows the top view schematic drawing of the wire bond model implemented in the EM simulator [13]. The model consists of two gold strips in air connected by vias at their edges. Each strip is divided into small subsections whose size can be adjusted depending on the desired accuracy. Wire bends at both ends of the wires are also modeled as edge vias.

The small triangles in Fig. 6(b) are the locations of the vias connecting the two strips along the periphery of the strips as well as vias to model the wire bend at both ends of the strips. For loose loop wire bonds, a more complicated EM model is required since the wire height above the ground is not constant and this variation needs to be taken into account. Other full 3-D EM simulators utilizing finite element and transmission line matrix [18], [19] algorithms are more suitable to simulate loose loop wire bonds since they allow more flexibility to draw 3-D geometries.

For practical applications such as that in circuit design incorporating parasitic effects caused by the wire bonds connecting a microwave integrated circuit to package pins, a simple, accurate and scalable lumped element model for wire bond is desired. Some research related to lumped element wire bond modeling [16] involves rigorous analysis based on the segmentation of the wire to derive the per unit length wire inductance. We propose a simple electrical wire model shown in Fig. 7. This model is suitable for short wires and consists of an ideal inductor  $L$  in series with a resistor  $R$  representing the wire inductance and loss due to metallization as well as radiation loss at the wire bends respectively. The capacitor  $C$  at the input and output ports represents the combination of substrate capacitance between the microstrip line onto which the wire is bonded to the ground plane and the wire capacitance to ground. This is assumed to be constant since all wires are bonded on the microstrip lines with identical configuration. The inductor  $L'$  at the input and output port represents end inductance caused by the bonds and is assumed to be constant as well for every configuration [17].

The values of the lumped elements in Fig. 7 are optimized [15] using Agilent's Microwave Design System (MDS) optimization engine to match the best and worst case wire bond

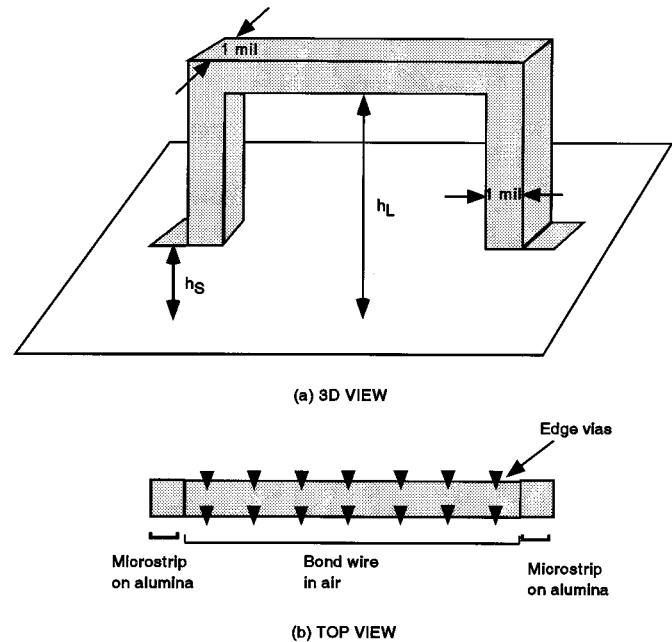


Fig. 6. Approximated geometry to (a) model wirebond implemented for (b) MoM simulation.

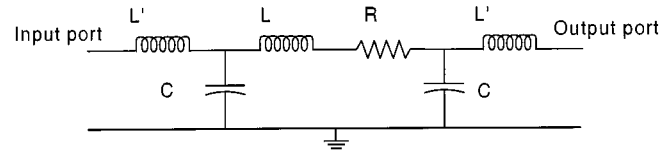


Fig. 7. Circuit schematic of wire bond electrical model.

performance for each configuration. The values of  $L'$  and  $C$  in Fig. 7 are independent of the length of the wire bond or the bonding process. Their values obtained from the optimization are 0.05 nH and 17.5 fF, respectively. The values for  $R$  are 0.2  $\Omega$  and 0.3  $\Omega$  for 15 and 25 mil wires, respectively. Since variation in both phase and magnitude of insertion loss is of more particular interest for most applications, specifically where the output magnitude and phase are critical, such as in balance-unbalance (balun), power combiner (divider) and phase shifter circuits, more weight is put on the insertion loss to provide better match to the measured results during the optimization [15]. The MoM simulations for tight loop wires show a good agreement to the measured results as indicated in Figs. 8 and 9 for the ball-crescent configuration. The simulated insertion loss is approximately the median between the best and worst case performance for each wire length. Even though the MoM simulation results are only superimposed with the measured results for the ball-crescent wire bonds, it is apparent that the results also lie in the median between the best and worst case insertion loss performance for the wedge wire bonds by comparison of the EM simulation results in Figs. 8 and 9 to the measured results in Figs. 4 and 5.

Variation caused by fabrication tolerances causes changes in the values of the lumped element model shown in Fig. 7. Since the bond shapes (both ball-crescent and wedge) are assumed to be identical, the element representing the parasitic due to the bonds which are the end inductance  $L'$  and capacitance  $C$  in

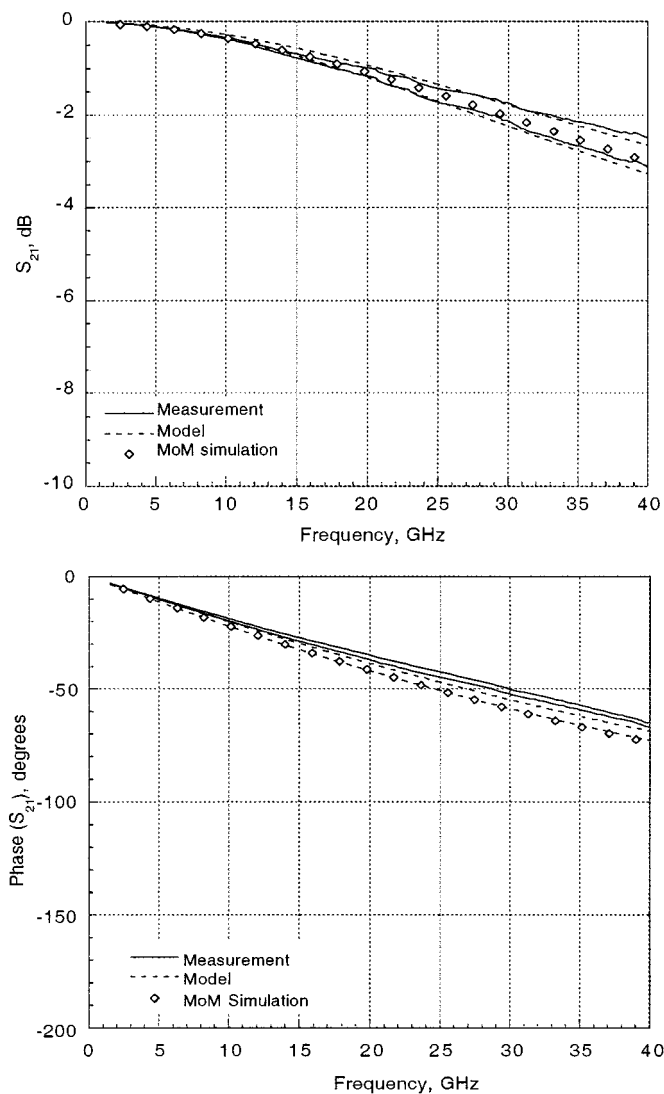


Fig. 8. Measured and modeled best and worst case insertion loss for 15 mil tight ball-crescent wire bond.

Fig. 7 for all wire lengths are constant. The only parameter change due to fabrication tolerance is the wire inductance  $L$ . Table II shows the summary of lower and upper bound wire inductance  $L$  for each configuration as well as the change in wire inductance indicated by  $\Delta L$  in the last column. The trends observed in the performance variation summarized in Table I are reflected in Table II. As discussed in Section III, the loose loop type is less repeatable than the tight loop wire bonds. Therefore, there is more variation in wire inductance for loose loop wire bonds as demonstrated by the larger value of  $\Delta L$  for the loose loop configuration of both ball-crescent and wedge configurations in Table II. Similarly, as previously stated, ball-crescent wire bonds are more repeatable and consequently have less change in wire inductance compared to the wedge configuration. This can be verified by comparing an average  $\Delta L$  of 0.055 nH and 0.09 nH for tight and loose ball-crescent, respectively to an average  $\Delta L$  of 0.11 nH and 0.12 nH for tight and loose wedge wire bonds, respectively. The measured and modeled insertion losses for the 15 and 25 mil tight ball-crescent wire bonds are given in Figs. 10 and 11, respectively.

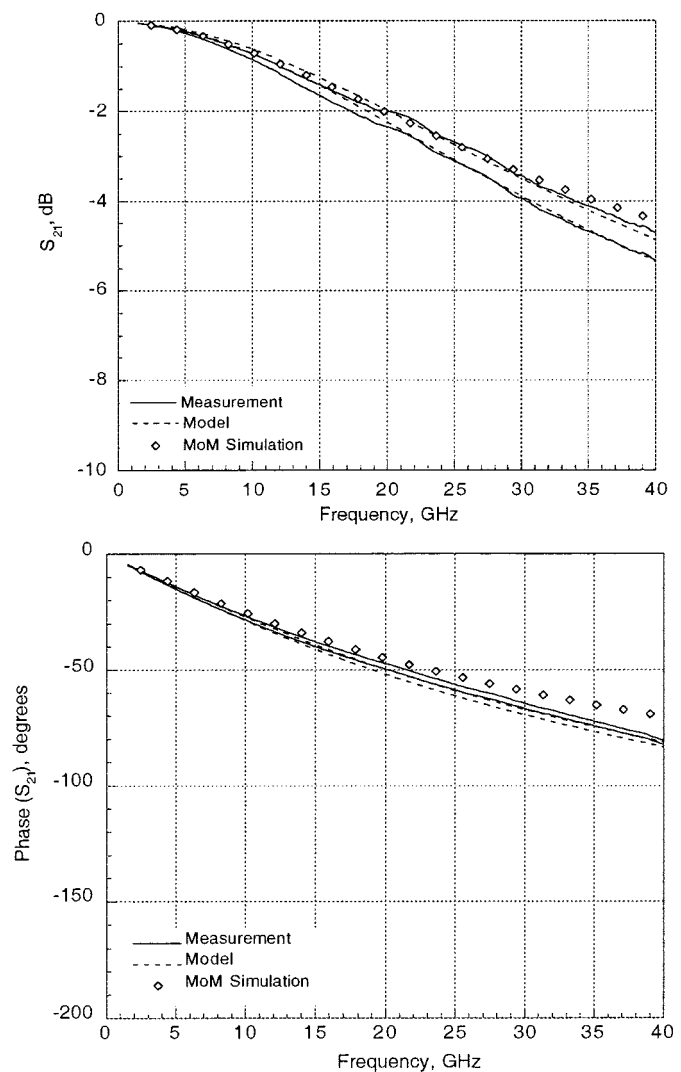


Fig. 9. Measured and modeled best and worst case insertion loss for 25 mil tight ball-crescent wire bond.

## V. A NEW RIBBON BOND INTERCONNECT TOPOLOGY

Bond wire interconnects can be analyzed as a lossy transmission line whose characteristic impedance is given by

$$Z_0 = \sqrt{\frac{R + j\omega L}{G + j\omega C}} \quad (1)$$

where  $R$ ,  $L$ ,  $G$  and  $C$  are the series resistance, series inductance, shunt conductance and shunt capacitance per unit length of the transmission line, respectively. It is desirable to obtain a low loss, 50- $\Omega$  matched bond-wire interconnects, since the typical input and output impedance of most microwave systems are 50- $\Omega$ . As mentioned in Section I, conventional bond wire configuration exhibits high characteristic impedance due to large  $L$  and small  $C$  in (1). Multiple bond wires placed in parallel [20], [21] reduce  $R$  and  $L$  and therefore, lower the  $Z_0$  and the insertion loss. A further improvement can be accomplished by the use of a ribbon bond which can eliminate the capacitive and mutual inductive coupling [21] typically present in the multi-wire topology. We propose a new ribbon bond interconnect traversing over air bent to close proximity to the ground plane. Such a

TABLE II  
WIRE INDUCTANCE VARIATION OF VARIOUS BOND-WIRE INTERCONNECT CONFIGURATIONS

Bond shape	Length (mils)	Loop Height	Lmin (nH)	Lmax (nH)	$\Delta L$ (nH)
Ball-crescent	15	Tight	0.38	0.44	0.06
Ball-crescent	25	Tight	0.60	0.65	0.05
Ball-crescent	15	Loose	0.45	0.54	0.09
Ball-crescent	25	Loose	0.74	0.83	0.09
Wedge	15	Tight	0.30	0.45	0.15
Wedge	25	Tight	0.53	0.60	0.07
Wedge	15	Loose	0.42	0.58	0.16
Wedge	25	Loose	0.77	0.86	0.09

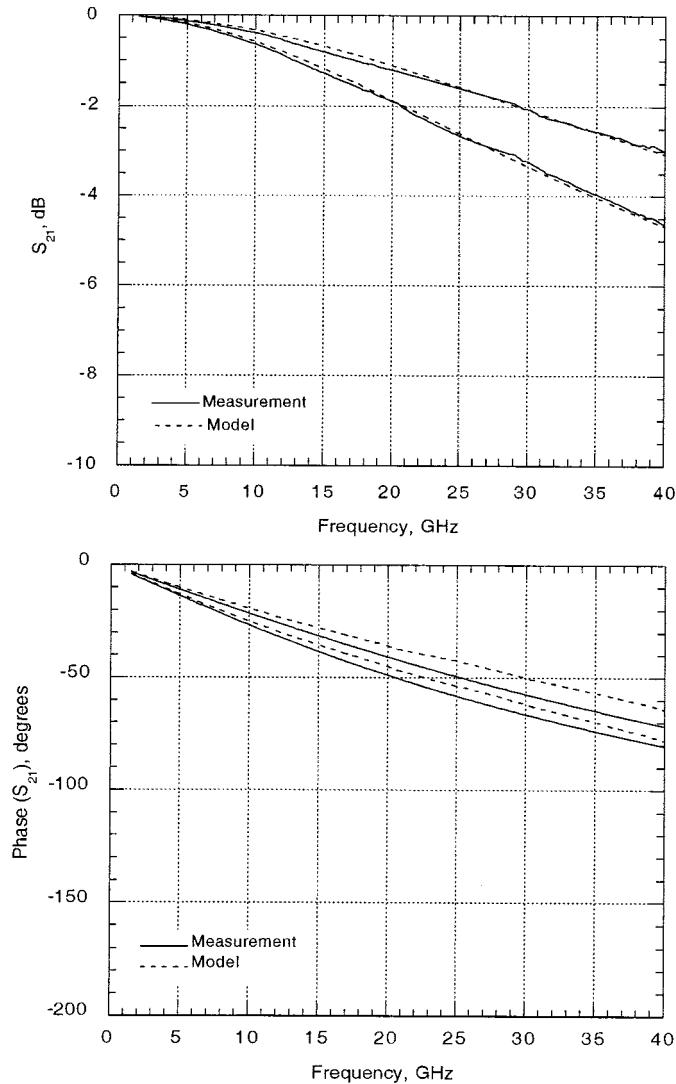


Fig. 10. Measured and modeled best and worst case insertion loss for 15 mil loose wedge wire bond.

topology has a small ribbon height above the ground plane and therefore, yields a larger  $C$ . In addition, a large ribbon width has a much less  $L$ . A combination of the two effects significantly reduce the  $Z_0$  of the interconnect.

We fabricated three different test structures to investigate and compare experimentally the performance of this new downward-bent ribbon topology. The first test structure (Type 1) consists of three arching wires bonded to the microstrip edge of

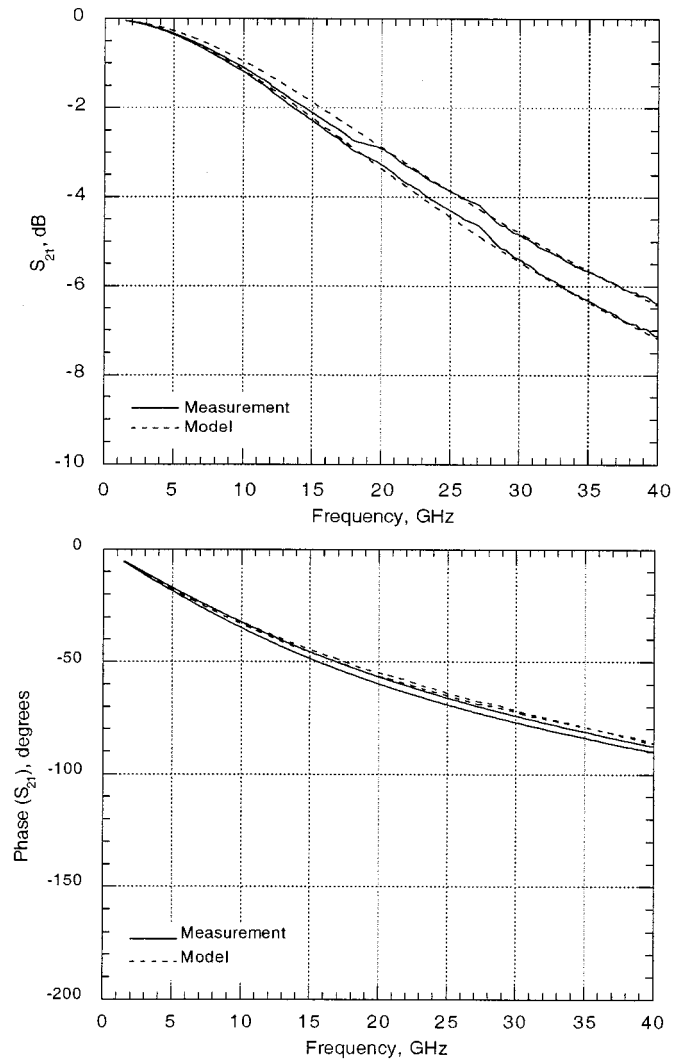


Fig. 11. Measured and modeled best and worst case insertion loss for 25 mil loose wedge wire bond.

the adapters as shown in Fig. 12(a). The gold ball-crescent type bond wires have a diameter of 1 mil and are fabricated using a thermosonic bonder. The second configuration (Type 2) shown in Fig. 12(b) is the same Type 1 except a 10 mil wide and 1 mil thick arching gold ribbon was used to connect the microstrip lines on the adapters. The third structure (Type 3) shown in Fig. 12(c) is the same as Type 2 but in this case, the ribbon was bent toward the ground plane as it traverses over air so that the height over the ground plane is much less than that of the first two configurations. A two-mil thick microscope film was used as a spacer gauge placed between the two adapters where the Type 3 ribbon was bonded as illustrated in the side view schematic in Fig. 12(c). It was used to control the ribbon height above the ground plane and more importantly, to ensure that the bonding process is repeatable. Once the ribbon was bonded, the microscope film was then removed. Thinner substrates such as a silicon substrate with thickness as thin as 6–8  $\mu\text{m}$  can be used as a spacer to enable the ribbon to be pulled even closer to the ground plane. The wires and ribbon were bonded as closely as possible to the end of the microstrip portion of the adapters. We performed TRL calibration from 1.5 GHz to 40

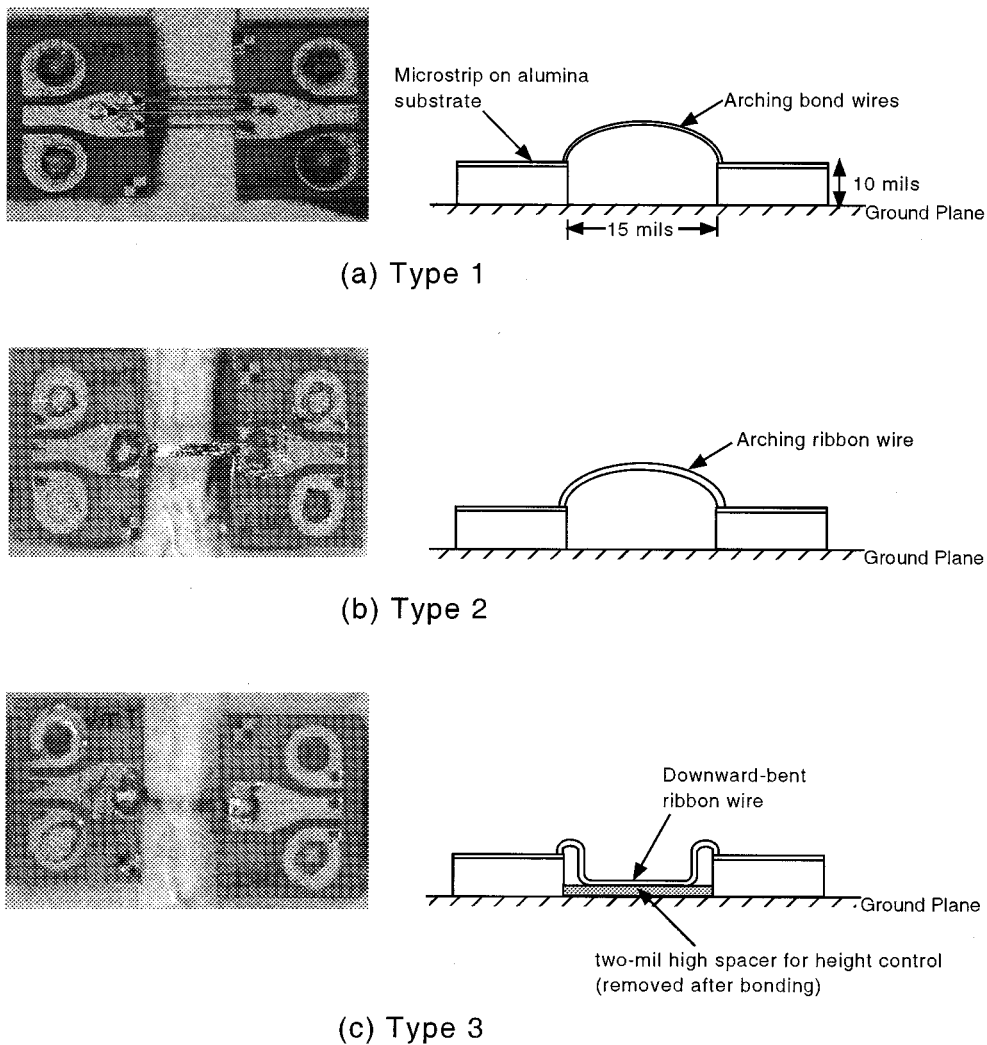


Fig. 12. Top view photographs (left column) and side view schematics (right column) of wire and ribbon bond test structures. (a) Type 1: Three gold bond wires arching on air. (b) Type 2: A single gold ribbon arching on air. (c) Type 3: A single gold ribbon bent to close proximity to the ground plane.

GHz to de-embed the adapters and established the reference plane at the microstrip end of the adapter so that the measured result contains only the structures under test. The  $S$ -parameter measurement of the test samples was then performed using HP8510B network analyzer after the calibration.

Figs. 13 and 14 show the measurement results of the three test structures. As indicated in Fig. 13, the return loss performance of Type 3 is superior to the other two types. A maximum improvement of more than 5 dB is observed at 40 GHz. Both Type 1 and Type 2 exhibit a return loss of 5 dB and 6 dB, respectively at 40 GHz as compared to more than 10 dB for Type 3. This corresponds to more than 65% reduction in the reflected power. Additional conductor and radiation loss is expected to occur in Type 3 due to a longer ribbon required to be bent closer to the ground plane as well as the discontinuities caused by the additional bending at both ends of the ribbon. However, this additional loss mechanism does not considerably degrade the insertion loss compared to both arching ribbon and multiple wire topologies. As observed from Fig. 14, Type 3 exhibits a maximum of 6% more insertion loss compared to the two other types. With the use of a 6- $\mu\text{m}$  thick Silicon substrate

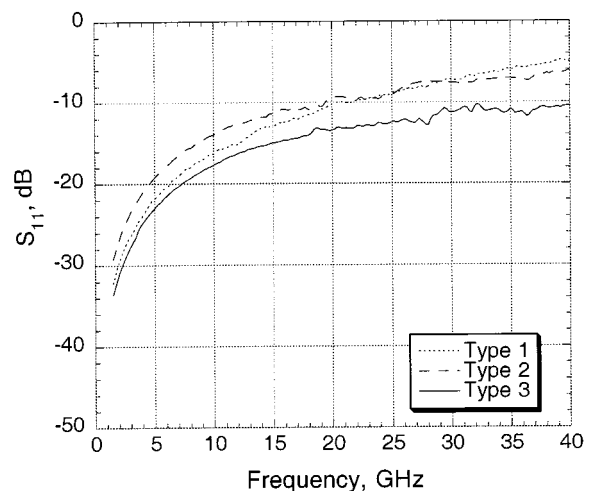


Fig. 13. Measured return loss of the three wire and ribbon bond test structures.

as the spacer, closer gap to the ground plane can be achieved to obtain a larger capacitance per unit length of the ribbon and thereby, lowering the  $Z_0$  and improving the return loss further.

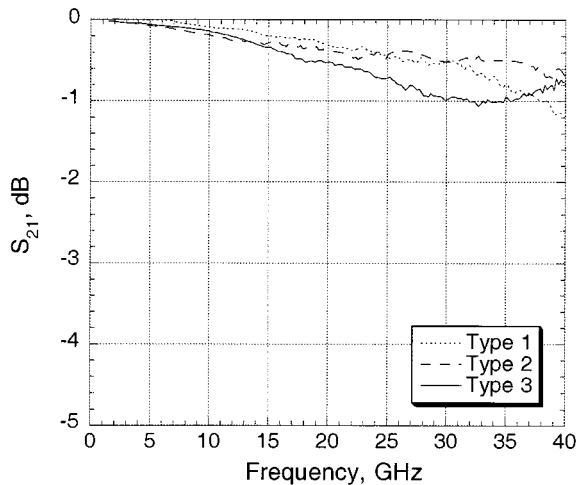


Fig. 14. Measured insertion loss of the three wire and ribbon bond test structures.

## VI. CONCLUSION

This paper thoroughly investigates the performance variation of different styles of wire bond interconnections typically used in microwave integrated circuits in terms of bond shapes, loop height and wire lengths using both experimental and simulation approaches. From a repeatability study, we demonstrate that the loose loop and the wedge type are less repeatable than the tight loop and the ball-crescent type, respectively. Also, a simple wide-band lumped-element model has been developed and verified with the measurement results to 40 GHz. The quantitative repeatability information presented in this paper is important in choosing what wire bond types to be used in a particular application, especially when uniformity of output magnitude and phase of the circuit are critical. Finally, we show the results of a new ribbon bond interconnect bent downward toward close proximity to the ground plane exhibiting a significantly better match with a comparable performance to the conventional topology.

## ACKNOWLEDGMENT

The authors would like to thank J. Mather and P. Feller, R. Collins Inc., as well as S. Halpern and M. Harris, Georgia Tech Research Institute, for fabricating the test structures.

## REFERENCES

- [1] R. Tummala and E. Rymaszewski, *Microelectronics Packaging Handbook*. New York: Chapman & Hall, 1997, vol. II, pp. 196–216.
- [2] R. H. Caverly, "Characteristic impedance of integrated circuit bond wire," *IEEE Trans. Microwave Theory Tech.*, vol. MTT-34, pp. 982–984, Sept. 1986.
- [3] H. Y. Lee, "Wideband characterization of typical bonding wire for microwave and millimeter-wave integrated circuits," *IEEE Trans. Microwave Theory Tech.*, vol. 43, pp. 63–68, Jan. 1995.
- [4] T. Itoh, "Overview of quasiplanar transmission lines," *IEEE Trans. Microwave Theory Tech.*, vol. 37, pp. 275–280, Feb. 1989.
- [5] G. Baumann, H. Richter, A. Baumgartner, D. Ferling, R. Heilig, D. Hollman, and H. Muller, "51 GHz front end with flip chip and wire bond interconnections from GaAs MMIC to a planar patch antenna," in *1995 IEEE MTT-S Dig.*, vol. 3, Orlando, FL, May 1995, pp. 1639–1642.
- [6] T. Krems, W. Haydl, H. Massler, and J. Rudiger, "Millimeter wave performance of chip interconnections using wire bonding and flip chip," in *1996 IEEE-MTT Dig.*, vol. 1, San Francisco, CA, June 1996, pp. 247–350.

- [7] A. Christ and H. L. Hartnagel, "Three dimensional finite difference method for the analysis of microwave device embedding," *IEEE Trans. Microwave Theory Tech.*, vol. 35, pp. 688–696, Aug. 1997.
- [8] L. Vietzorreck and R. Pregla, "3-D modeling of interconnects in MMIC's by the method of lines," in *1996 IEEE MTT-S Dig.*, vol. 1, Orlando, FL, June 1996, pp. 347–350.
- [9] R. B. Marks, "A multiline method of network analyzer calibration," *IEEE Trans. Microwave Theory Tech.*, vol. 39, pp. 1205–1215, July 1991.
- [10] C. A. Hoer, "Choosing line lengths for calibrating network analyzers," *IEEE Trans. Microwave Theory Tech.*, vol. 31, pp. 76–78, Jan. 1995.
- [11] A. Pham, J. Laskar, and J. Schappacher, "Development of on-wafer microstrip characterization techniques," in *47th IEEE-ARFTG Dig.*, San Francisco, CA, pp. 85–94.
- [12] "Applying the HP8510B TRL Calibration for Non-Coaxial Measurements," Product Note 8510-8, Hewlett Packard Co., 1987.
- [13] *EM User Manual*, Sonnet Software Inc., Liverpool, NY.
- [14] R. F. Harrington, *Field Computation by Moment Methods*, 1993.
- [15] "HP Microwave and RF Design Systems, Component Catalog," vol. 3, Microwave Library Components (Distributed).
- [16] S. M. Riad, W. Lu, I. Salama, A. Elshabini, and M. Rachlin, "Plastic package modeling and characterization at RF/microwave frequencies," in *Proc. 4th Int. Symp. Exhibition Adv. Packag.*, Mar. 1998.
- [17] HP Microwave and RF Design Systems, "Designer's Task Reference: Simulating and Optimizing Circuit Performance," Tech. Rep., vol. 4, 2001.
- [18] *HP High Frequency Structure Simulator Reference Manual*, Hewlett Packard, 2001.
- [19] *MicroStripes™ Microwave Field Simulator User's Manual*, KCC, Nottingham, U.K., 2001.
- [20] F. Alimenti, P. Mezzanotte, L. Roselli, and R. Sorrentino, "Equivalent circuit for the double bonding wire interconnection," in *1999 IEEE MTT-S Dig.*, vol. 2, Anaheim, CA, June 1999, pp. 633–636.
- [21] —, "Multi-wire microstrip interconnections: A systematic analysis for the extraction of an equivalent circuit," in *1998 IEEE MTT-S Dig.*, vol. 3, Baltimore, MD, June 1998, pp. 1929–1932.

**Albert Sutono** (M'96) received the B.S. degree from Iowa State University, Ames, in 1996, and the M.S. and Ph.D. degrees from the Georgia Institute of Technology, Atlanta, in 1999 and 2001, respectively, all in electrical engineering.

He has published over 30 peer-reviewed journal and conference papers in the area of RF/microwave/millimeter wave circuits and packaging. Since February 2001, he has been with RF Solutions, Inc., Atlanta, GA.

**N. Gio Cafaro** (M'00) was born in Tampa, FL, in 1974. He received the B.S. degree in electrical engineering from the University of South Florida, Tampa, in 1998 and the M.S. degree in electrical engineering from the Georgia Institute of Technology, Atlanta, in 1999.

In 2000, he joined Motorola Labs, Plantation, FL, where he has since worked on broadband communications circuits including distributed power amplifiers. He is currently working on mixed-signal IC designs for direct digital synthesizers.

**Joy Laskar** (M'91) received the B.S. degree (with highest honors) in computer engineering from Clemson University, Clemson, SC, in 1985, and the M.S. and Ph.D. degrees in electrical engineering from the University of Illinois, Urbana-Champaign, in 1989 and 1991, respectively.

Prior to joining the Georgia Institute of Technology (Georgia Tech), Atlanta, in 1995, she held faculty positions at the University of Illinois and the University of Hawaii. At Georgia Tech, she is currently the Chair for the Electronic Design and Applications Technical Interest Group, the Director of Research for the state of Georgia's Yamacraw Initiative, and the NSF Packaging Research Center System Research Leader for RF and Wireless. His research has focused on high frequency IC design and their integration. At Georgia Tech, she heads a

research group of 25 members with a focus on integration of high frequency electronics with optoelectronics and integration of mixed technologies for next generation wireless and optoelectronic systems. His research is supported by over 15 companies and numerous federal agencies including: DARPA, NASA and NSF. She is a co-organizer and Chair for the Advanced Heterostructure Workshop, serves on the IEEE Microwave Theory and Techniques Symposia Technical Program Committee, and is a member of the North American Manufacturing Initiative Roadmapping Committee. She has published over 100 papers, numerous invited talks, and has ten patents pending. She is co-founder of the broadband wireless company RF Solutions, Inc., and co-founder of the next generation optical technology company Quellan, Inc. In July 2001, she was named the Petit Chair Professor of Electronics in the School of Electrical and Computer Engineering, Georgia Tech.

Dr. Laskar received the 1995 Army Research Office's Young Investigator Award, the 1996 National Science Foundation's CAREER Award, the 1997 NSF Packaging Research Center Faculty of the Year Award, the 1998 NSF Packaging Research Center Educator of the Year Award, the 1999 IEEE Rappaport Award (Best IEEE Electron Devices Society Journal Paper), the 2000 IEEE MTT IMS Best Paper award, and the 2001 Georgia Tech Faculty Graduate Student Mentor of the Year Award.

**Manos M. Tentzeris** was born in Piraeus, Greece. He received the Diploma degree in electrical engineering and computer science (with high honors) from the National Technical University, Athens, Greece, and the M.S. and Ph.D. degrees in electrical engineering and computer science from the University of Michigan, Ann Arbor.

He is currently an Assistant Professor with the School of Electrical and Computer Engineering, Georgia Institute of Technology (Georgia Tech), Atlanta. His research is concerned with the development of novel numerical time-domain techniques and the application of multiresolution analysis principles to the analysis and design of microwave circuits used in wireless communications and VLSI geometries. He has published more than 60 papers in refereed journals and conference proceedings and three book chapters. He has helped develop academic programs in highly integrated packaging for RF and wireless applications, microwave MEM's modeling, SOP-integrated antennas, low-crosstalk compact finite-ground coplanar waveguides (FGC) circuits and adaptive numerical electromagnetics (multiresolution algorithms). He is the RF Thrust Leader of Georgia Tech's NSF-Packaging Research Center and the leader of the Novel Integration Techniques Subthrust of the Broadband Hardware Access Thrust of the Yamacraw Initiative of the State of Georgia.

Dr. Tentzeris received the 2001 ACES Conference Best Paper Award, the 2000 NSF CAREER Award, and the 1997 Best Paper Award of the International Hybrid Microelectronics and Packaging Society. He was also the 1999 Technical Program Co-Chair of the 54th ARFTG Conference, Atlanta, GA, and he is the Vice-Chair of the RF Technical Committee (TC16) of the IEEE CPMT Society.